8-2011

Streambank Erosion and Instability Induced by Groundwater Seepage

Taber L. Midgley
Oklahoma State University, taber.midgley@okstate.edu

Garey A. Fox
Oklahoma State University, gafox2@ncsu.edu

Glenn V. Wilson
USDA Agricultural Research Service, glenn.wilson@ars.usda.gov

Derek M. Heeren
University of Nebraska-Lincoln, derek.heeren@unl.edu

Andrew Simon
USDA Agricultural Research Service, andrew.simon@ars.usda.gov

See next page for additional authors

An ASABE Meeting Presentation

Paper Number: 1110988

2950 Niles Road, St. Joseph, MI 49085-9659, USA
269.429.0300 fax 269.429.3852 hq@asabe.org www.asabe.org

Streambank Erosion and Instability Induced by Groundwater Seepage

Taber L. Midgley, Master of Science Student

Oklahoma State University, 117 AGH, Stillwater, OK 74078, taber.midgley@okstate.edu

Garey A. Fox, Associate Professor

Oklahoma State University, 111 AGH, Stillwater, OK 74078, garey.fox@okstate.edu

Glenn V. Wilson, Research Hydrologist/Soil Physicist

USDA Agricultural Research Service, 598 McElroy Dr., Oxford, MS 38655, glenn.wilson@ars.usda.gov

Derek M. Heeren, Research Engineer

Oklahoma State University, 111 AGH, Stillwater, OK 74078, derek.heeren@okstate.edu

Andrew Simon, Geologist/Geomorphologist

USDA Agricultural Research Service, 598 McElroy Dr., Oxford, MS 38655, andrew.simon@ars.usda.gov

Eddy J. Langendoen, Research Hydraulic Engineer

USDA Agricultural Research Service, 598 McElroy Dr., Oxford, MS 38655, eddy.langendoen@ars.usda.gov

Written for presentation at the
2011 ASABE Annual International Meeting
Sponsored by ASABE
Galt House
Louisville, Kentucky
August 7 – 10, 2011

Abstract. *Excessive sediment is one of the most common surface water pollutants. It diminishes water quality and destroys aquatic habitat. Streambank erosion is known to be a major source of*

sediment in streams and rivers, contributing as much as 80% of the total sediment load in some watersheds. Little work has been done to study the effects of seepage on streambank erosion and failure. Prior research, primarily in the laboratory under well-defined and controlled conditions, has examined seepage as a mechanism for bank erosion, but more needs to be done to validate conclusions derived from the laboratory with field data. This project studied a streambank on Dry Creek (a tributary to Little Topashaw Creek) located in Chickasaw County, Mississippi. The bank was previously observed to produce seepage even during dry summer months. This creek is a deeply incised stream in the Yalobusha Watershed with near 90 degree banks. The creek flows through alluvial plains under cultivation and surrounded by forested areas. Excess sediment has been identified as the main water quality issue in the watershed with gullies and banks being the main sources. Watershed geology is characterized by silt loam and clay loam with a more conductive loamy sand between the loam and an underlying cohesive layer. The site was initially instrumented with a network of tensiometers and observation wells. Groundwater conditions and bank erosion were monitored for several weeks, followed by an induced seepage experiment. A trench installed 2.8 m from the edge of the bank and approximately 2 m below ground surface was used to provide a constant head for groundwater flow in the near-bank area. The bank face was outfitted with a seepage collection device that measured seepage flow rate and sediment transport. Groundwater conditions were again monitored by the tensiometer and observation well network. Experiments consisted of a trench injection at a constant head and observations of flow rates, erosion rates, soil-water pressures, and water table elevations. Flow rates varied from 0.004 L/min to 1.16 L/min at different locations on the bank. It was observed that the seeps experienced 'self-healing' erosion in which upper layer cohesive soil failures blocked further particle mobilization. One experiment simulated fluvial erosion removing the failed material, thereby, resulting in combined erosion rates of over 6000 g/min. Seepage erosion could be a dominate mechanism of streambank failure where the self-healing process is not occurring.

Keywords. Bank erosion, Seepage erosion, Subsurface flow, Sapping, Streambank stability

Introduction

Bank erosion has been neglected in quantifying sediment yield in watersheds until the 1970's (Lawler et al., 1997) but may be the source of 54-80% of sediment yield in some cases (Wilson et al., 2008). Two mechanisms are typically credited for the bulk of streambank erosion: fluvial erosion and mass wasting due to bank instability. Fluvial erosion occurs when excess shear stress caused by stream flow provides enough force to cause the detachment and removal of sediment particles or aggregates of particles from the bank face. In cohesive banks this process is influenced by the mineralogy, particle size, moisture content, and a balance of lift, drag, weight, and friction forces (Lawler et al., 1997). In non-cohesive banks, entrainment depends on a balance of forces with lift and drag driving motion and friction and gravity resisting (Lawler et al., 1997). Mass wasting occurs when an imbalance of gravity and friction/cohesion forces exist on a block of bank material. The resisting forces are governed by a modified Mohr-Coulomb equation in which shear strength depends on effective cohesion of the soil, normal stress caused by block weight, soil-water pressure, and the soil's angle of internal friction. Driving forces include weight which increases with bank saturation. Failure also depends on the plane over which driving and resisting forces act. This plane is referred to as the failure plane. As the failure plane is shortened by fluvial undercutting, bank steepening, or tension cracks, the driving stresses exerted on the plane increase.

Another mechanism, subsurface flow, may be equally important in some cases, but is neglected in many cases. Subsurface flow can cause erosion and bank instability in several specific mechanisms (Fox and Wilson, 2010). These mechanisms include soil-water pressure, seepage gradient forces, seepage erosion, and pipe erosion.

Bank stability of unsaturated soils is governed by the modified Mohr-Coulomb equation:

$$s = [c' + (\sigma_n - u_w)\tan\varphi'] + [(u_a - u_w)\tan\varphi^b] \quad (1)$$

where s is the shear strength, c' is the effective cohesion, σ_n is normal stress, u_w is the soil-water pressure, φ' is the internal angle of friction, u_a is the soil-air pressure, and φ^b is the friction angle associated with the relationship between shear strength and matrix suction (Fredlund and Rahardjo, 1993). Negative soil-water pressures increase the second bracketed term of the modified Mohr-Coulomb equation, creating an apparent cohesion. When water infiltrates the bank from either recharge or precipitation, the soil-water pressures increase reducing the apparent cohesion (Fox and Wilson, 2010). Rinaldi et al. (2004) studied the effects of soil-water pressure on bank stability for four years on the Sieve River in Italy. They found that even without fluvial undercutting a slight decrease in apparent cohesion due to soil-water pressure is enough to cause bank failure.

Iverson and Major (1986) noted that a seepage force vector is responsible for destabilizing hillslopes subjected to subsurface flow and claimed seepage forces played a bigger role on slope destabilization than excess soil-water pressures. They found that stability of hillslopes subjected to seepage depend on three factors: the ratio of the seepage force magnitude to gravitational force magnitude, the angle θ-φ where θ is the bank angle and φ is the internal angle of friction, and the angle λ-φ where λ is the seepage vector angle measured from surface normal vector. This mechanism can cause Coulomb failure as described above or liquefaction, the complete loss of shear strength in the soil (Fox and Wilson, 2010). Hagerty (1991) recognized that even with substantial research, computer models, and laboratory experiments on the effects of seepage erosion, there was a lack of application and understanding of seepage processes.

For failure to occur, the hydraulic gradient of the seepage must be substantial enough to overcome all the resisting forces acting on the soil particles, such as interlocking, interparticle friction, cohesion, cementation, binding by roots, and gravity (Hagerty, 1991). These types of failures are often referred to as 'pop out' or tension failures. Lobkovsky et al. (2004) showed that the seepage force is proportional to the hydraulic gradient with the following relationship:

$$SF = \rho g \frac{\partial h}{\partial y} \quad (2)$$

where *SF* is the seepage force per unit area, ρ is the fluid density, *g* is acceleration due to gravity, *h* is the hydraulic head and *y* is the distance over which *h* acts (Fox and Wilson, 2010). Chu-Agor et al. (2008) conducted laboratory experiments in order to analyze this type of erosion. They found that if the soil was weak, i.e. the soil resistive forces cannot withstand the seepage gradient forces, a 'pop out' failure would occur. When the resistive forces (cohesion) are high enough to resist a pop out failure, the possibility of concentrated seepage with high velocity occurs leading to particle mobilization as described in the following section.

Wilson et al. (2007) noted that seepage erosion, i.e. mobilization of particles entrained in the seepage exfiltrating a bank face, was causing undercutting of deeply incised streambanks in Mississippi. Hagerty et al. (1981) made similar observations along the Ohio River and termed this process internal erosion, while others (Richards and Reddy, 2007) use the term backwards erosion for this form of piping. In contrast, internal erosion is almost always associated with the erosion of the inside walls of a preferential flow paths, e.g. macropores or soil pipes (Fox and Wilson, 2010; Wilson et al., 2011). Seepage erosion is generally attributed to layers of contrasting hydraulic properties within the banks and terraces in which a less permeable layer causes lateral flow through a more conductive, often non-cohesive, layer above. Water flowing through the higher hydraulic conductivity layer causes seepage erosion, particle entrainment, at the bank face. An undercut develops as the non-cohesive layer erodes away and eventually the overlying cohesive layers fail (Hagerty et al., 1981; Fox et al., 2007). This process was attributed by Hagerty (1981) to be one of the dominate mechanisms causing bank retreat on the Ohio River, particularly during time periods with high precipitation.

Rulon et al. (1985) developed and validated a finite element model for analyzing groundwater seepage in a hillslope with impeding (lower hydraulic conductivity) layers. Flow was modeled as steady state, saturated-unsaturated flow through a 2D heterogeneous region. This model was validated by Rulon et al. (1985) with a laboratory experiment using a plexiglass sand tank filled with medium sand using fine sand as the impeding layer. Inflow into the physical model was simulated by a rainfall simulator. The physical and finite element model demonstrated that concentrated exfiltration would occur just above the impeding layer. The exfiltration strongly depended on the position of the impeding layer and the hydraulic conductivity ratio.

Similar to fluvial erosion, seepage flow can cause shear stresses to overcome the frictional and gravitational forces resisting movement of particles. Chu-Agor et al. (2008) conducted multiple laboratory experiments observing seepage erosion undercutting and found that when the bank could resist the seepage gradient forces and the seepage was concentrated, particle mobilization was initiated. Development and size of the undercut depended on the bulk density of the soil, which influences hydraulic conductivity, cohesion, internal angle of friction, and critical hydraulic gradients to induce seepage particle mobilization. Sapping refers to the mass failure of banks as a result of seepage erosion undercutting (Fox and Wilson, 2010). A progression of seepage undercutting and sapping can be seen in figure 1.

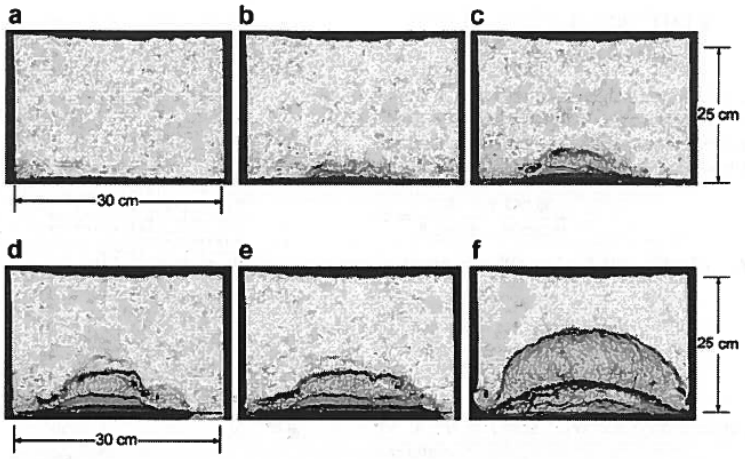

Figure 1. Seepage erosion undercutting and sapping experiment progression: (a) original bank face, (b) to (e) seepage undercutting, and (f) sapping failure (Chu-Agor et al. 2008).

Seepage erosion is difficult to recognize as an active factor in bank erosion for many reasons. Hagerty (1991) and Fox and Wilson (2010) list several:

- Seepage erosion is subtle.
- Seepage erosion is intermittent. Seepage erosion is a very complex mechanism, and many different conditions can cause substantial seepage erosion after one storm event, but negligible erosion after a different storm event.
- Undercutting of streambanks may be misinterpreted as resulting from fluvial erosion.
- Seepage erosion occurs in combination with other bank erosion mechanisms which may hide evidence of seepage erosion. For example, sapping erosion may cause an undercut bank to fail that would remove evidence of earlier undercutting and/or cover the original seepage face with failed material.

The American Society of Civil and Environmental Engineers Task Committee on Hydraulics, Bank Mechanics, and Modeling of River Adjustments recommends better methods of predicting streambank erosion need to be developed (ASCE, 1998).

The objective of this research was to investigate the various mechanisms of seepage erosion under field conditions to verify laboratory predictions of seepage undercutting. It is hypothesized that subsurface processes play a major role in streambank stability and erosion.

Materials & Methods

Field Site and Site Characterization

Dry Creek, located in Chickasaw County, Mississippi, is a tributary to Little Topashaw Creek (LTC), an experimental subwatershed of the Topashaw Canal CEAP watershed in Mississippi, Wilson et al. (2008). Evidence of seepage erosion was noticed at several locations along Dry Creek and LTC in the form of undercutting and deposition/flow patterns in the soil. This creek is a deeply incised stream with near 90^{o} banks that flow through alluvial plains under cultivation and surrounded by forested areas. Excess sediment has been identified as the main water quality issue in the watershed with gullies and banks being the main sources (Wilson et al.,

2008). General watershed geology is characterized by silt loam and clay loam overlying a more conductive loamy sand which overlies a cohesive layer (Fox et al., 2006). Wilson et al. (2007) provides extensive analysis of soil properties on the banks of the LTC.

A site survey of Dry Creek was conducted using total station equipment and known monuments established from previous studies. Elevations above sea level of relevant locations are indicated in figure 2. The strongest evidence of seepage was located 3.5 m below the top bank while the baseflow water elevation was located 6.5 m below top bank.

Soil property measurements were acquired to quantify strength parameters. Soil samples were collected from various depths on the bank face and trench. Borehole shear tests were conducted at various depths in the soil profile using an Iowa Borehole Shear Test Model A104.2. Tests were conducted at three different locations and six different depths (1.0, 1.5, 2.0, 2.5, 3.0, and 4.0 m depths). Tests consisted of boring a hole to the desired depth and inserting the BST shear head. The shear head was attached to a dynamometer by a pull rod. CO_2 was used to pressurize the shear head against the sides of the bore hole (normal stress). Depending on the location, soil water pressures were measured at the time of the shear tests. Finally a crank was used to apply upward pressure on the shear head (shear stress) until failure. The normal stress and corresponding shear stress at failure was plotted to create the failure envelope. The test was repeated at four different increasing normal stresses at each depth to derive the apparent cohesion and internal angle of friction. To estimate an effective cohesion and effective internal angle of friction, the tensiometer data were used to estimate matric suction, as shown in equation (1).

Site setup included installation of an injection trench, observation wells, and tensiometers. The trench was installed 2.8 m from the nearest point on the bank with a length of 2.4 m, a width of 0.6 m, and depth of 2 m (fig. 3). A wood frame was constructed with plywood walls and inserted into the trench (fig. 4). The plywood on the stream side of the frame had a pattern of holes drilled through it in order to allow infiltration into the soil profile. Gravel filled the bottom foot of the trench and around the outside of the bank side of the frame.

Nine observation wells were installed at two different depths (2 m and 4.3 m). Wells were installed in three columns from the trench to the bank edge (fig. 5). Each well was equipped with an Onset® Hobo Data logger for recording water depth and temperature. Sixteen UMS T4 tensiometers were installed between the trench and the bank edge at multiple depths (fig. 6). Additionally, six 30 cm T5 tensiometers were installed into the bank face at multiple elevations below the top bank. As shown in figure 6, the tensiometers are referred to by their row (trench, middle, bank, or face), then their column (left, middle, right), and finally their depth in cm. For example, BM250 refers to the T4 tensiometer in the row nearest the bank, middle column, at 250 cm depth.

Figure 2. Dry Creek bank for seepage experiments. Photo taken January 19, 2011 after kudzu was removed. Locations of evidence of seepage are indicated by circles.

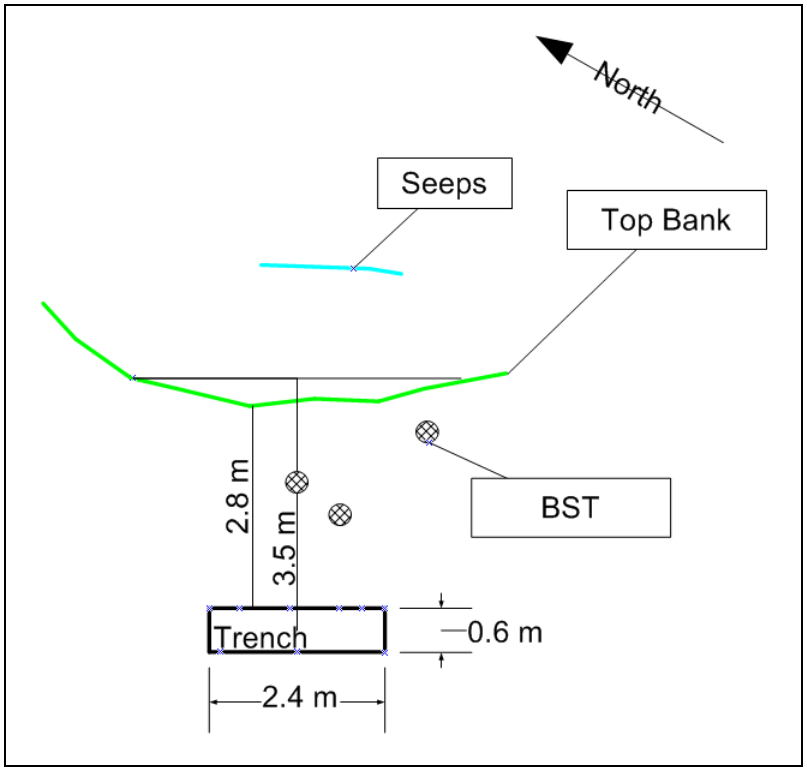

Figure 3. Trench location and dimensions relative to surveyed top bank profile (aerial view). Locations of borehole shear tests (BST) are indicated.

Figure 4. Trench frame installation for induced seepage experiments. The trench was located 2.8 m from the bank face.

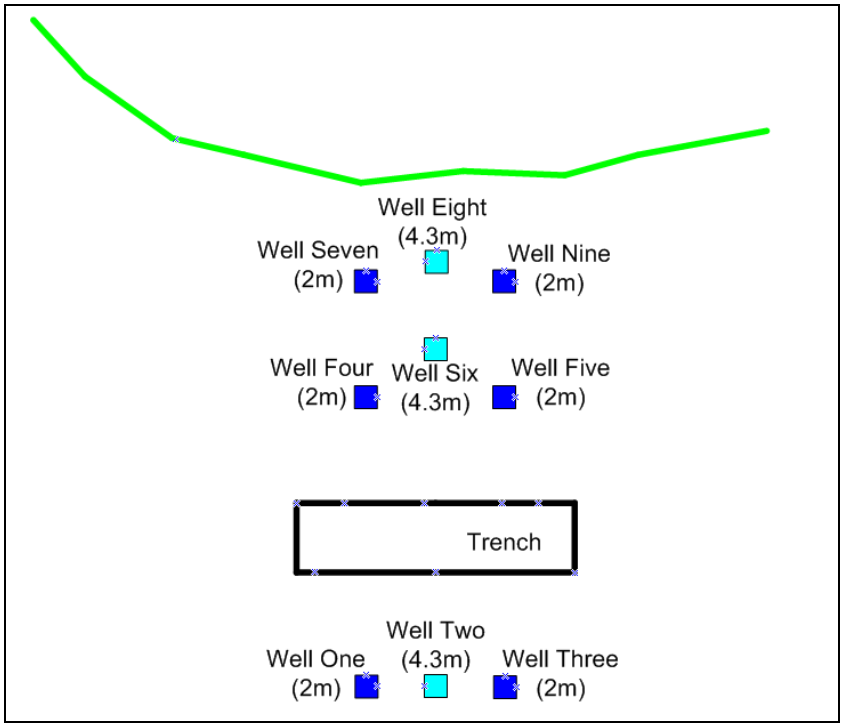

Figure 5. Well locations and depths relative to surveyed top bank profile (aerial view).

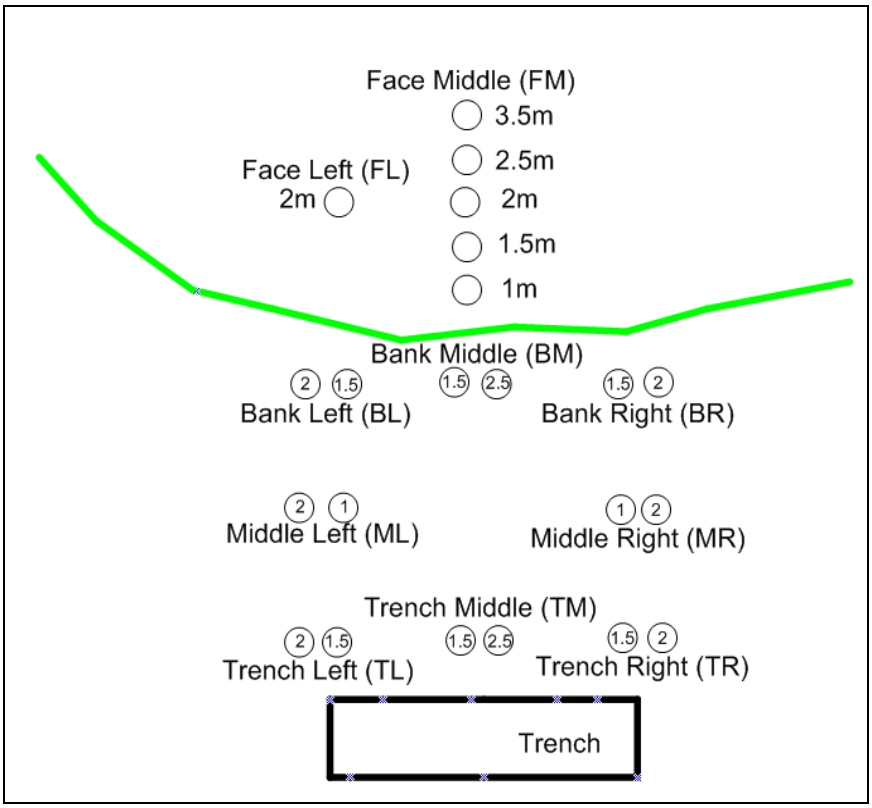

Figure 6. Tensiometer locations. For tensiometers located between trench and bank edge, the number indicates the tensiometer depth in meters. Tensiometers beyond the bank edge are 30 cm "pen" tensiometers installed horizontally into the bank face at the depth indicated.

Seepage Collection and Flowrate Measurement System

In order to collect data on seep flow and erosion rates, a system had to be designed which could easily catch water and eroded soil from a localized seep. Several seepage collection pans were constructed of varying widths. A pan was driven into the bank below the seepage location and secured. The pan routed seepage and entrained particles to a PVC pipe which led down the bank to collection vessels (fig. 7). Two methods were used to obtain flow and erosion rate measurements. For high flow seeps, a 5 gallon (18.9 L) bucket was placed at the end of the PVC pipe. This bucket was allowed to fill for a set amount of time, at the end of which the bucket was weighed. Finally, the contents of the bucket would be manually stirred to evenly distribute all sediment in the water and a representative sample taken. This sample was later analyzed in the lab for sediment concentrations. Using the weights of the buckets plus the sediment concentrations, flow and erosion rates were derived. For low flow rate seeps, a small sample bottle collected the seepage from the end of the PVC pipe after which the entire sample was taken to the lab for flow and erosion rate determination.

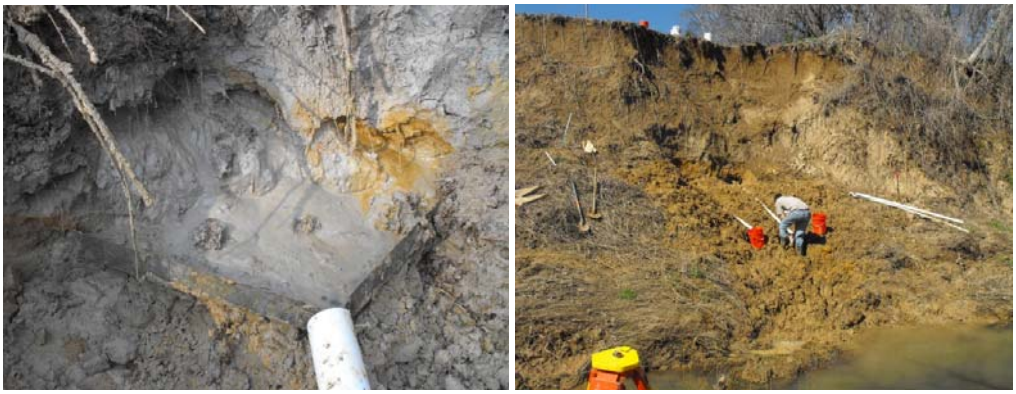

Figure 7. Installed seepage pan during seepage experiment (left) and view of bank and collection system below two active seeps.

Seepage Experiments

The trench was filled and not held at a constant head on 3/15/2011 and 3/16/2011 as the goal was to pre-wet the bank to provide a good potential for seepage once the experiments started. Actual seepage experiments started on 3/18/2011 and continued until 3/20/2011 (table 1). Seepage occurred in three major locations, referred to as East Seep (ES), Middle Seep (MS), and West Seep (WS), as indicated in figure 8. Samples were collected from each of these seeps in one of the two methods described above.

An 'experiment' refers to a time period in which samples and data were collected from a given seep. Five seepage experiments were conducted: one on the east seep, one on the middle seep, two on the west seep, and one longer term experiment where the bank was observed and trench filled but no samples were collected. Most experiments were started first by filling and maintaining a constant head in the trench and second by digging a vertical face at the seep location. As seepage began mobilizing the sediment and flowing into the collection pan, sapping failure would occur in the upper cohesive soil. For the second west seep experiment (WS2), sapped and seeped material were simultaneously collected separately as best as possible. For all other experiments, the failed material was allowed to accumulate in the pan or drain with the seepage on its own. Periodic measurements of the undercuts were recorded to monitor undercut growth.

Table 1. Summary of events and experiments conducted.

Experiment Label	Description	Trench Filled	Trench held Constant until
	Trench filled to wet soil profile	3/15/2011 11:10	Allowed to drain
	Trench filled to wet soil profile	3/15/2011 12:30	Allowed to drain
	Trench filled to wet soil profile	3/16/2011 11:20	Allowed to drain
MS (Middle Seep)	Seepage experiment	3/18/2011 11:20	3/18/2011 19:20
ES (East Seep)	Seepage Experiment	3/18/2011 11:20	3/18/2011 19:20
WS1 (West Seep 1)	Seepage Experiment	Trench not filled	
WS2 (West Seep 2)	Seepage Experiment with eroded soil removal	Trench not filled	
LTE (Long Term Exp.)	Seepage Experiment w/o sampling	3/19/2011 11:40	3/20/2011 0:00
LTE (Long Term Exp.)	Seepage Experiment w/o	3/20/2011 9:40	3/20/2011 14:30

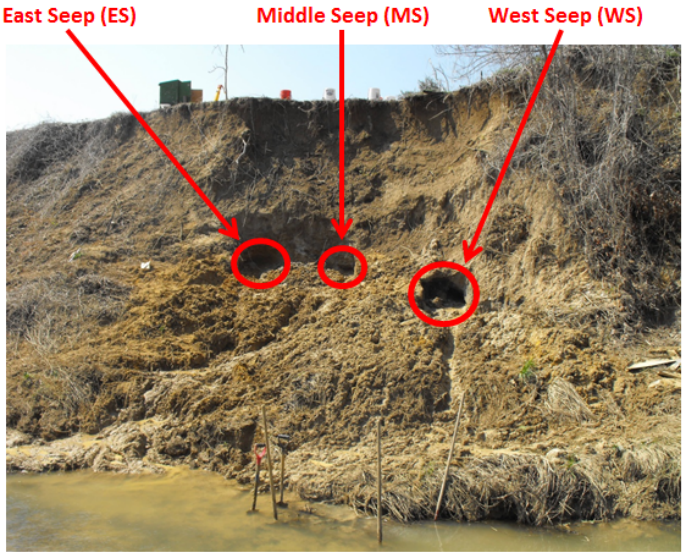

Figure 8. Locations and naming conventions of seeps on the Dry Creek bank.

Results & Discussion

Soil Properties

Before any experiments, the bank consisted of a steep upper cohesive face and a gradually sloped toe of cohesive material overlying a sand layer. It can be assumed that this cohesive material was deposited on the toe by mass wasting events in the past. This cohesive soil capped the underlying sandy layer, preventing both fluvial undercutting and seepage erosion undercutting during the study period. Before this material was removed, seepage only occurred when a high water table provided enough head to drive seepage through this material. When natural high water table events caused seepage through the toe, erosion due to seepage was limited by the cohesive nature of the deposited soil. Seepage was observed before the experiments near the bottom of the toe but caused little particle mobilization or pop out failures. Once the cohesive material of the upper toe was removed for the experiments and the sandy layer was exposed, seepage erosion began immediately.

In terms of bank stratigraphy, it was observed that the sand (seepage) layer was inclined, rising higher in elevation as one moved east. Because the seepage face in the west seep was lower in elevation than the east seep, the west seep had much higher flow rates and erosion rates, as discussed below. Borehole shear tests illustrated the variability in streambank c' and φ' with depth (table 2). Similar to LTC streambanks (Wilson et al., 2007), the streambank consisted of less cohesive sand layers underlying more cohesive loams. The borehole shear test data confirmed the presence of the less cohesive sands with apparent cohesions of 3.3 kPa approximately 3.0-3.5 m below ground surface. Apparent cohesions in the loam and sandy layer above the sand seep layers ranged between 2.17 and 14.28 kPa (table 2).

Table 2. Summary of borehole shear test results.

Depth of Test (m)	Friction Angle (deg)	Matric Suction (kPa)	Cohesion due to matric suction (kPa)	Effective Cohesion (kPa)	Apparent Cohesion (kPa)	Observed Soil Type
1.0	18.76	6.2	1.09	7.89	9.07	Loam
1.5	28.18	4.8	0.85	9.19	10.04	Loam
2.0	32.31	5	0.88	1.29	2.17	Loam
2.5	24.54	0	0	14.28	14.28	Sandy
3.0	29.37	0	0	3.33	3.33	Sand w/ layers of loam
4.0	21.28	0	0	9.56	9.56	Sand

Observation Wells

The deep 4.3 m wells responded fast, within an hour, to establishing a head in the trench (fig. 9). Well 2, located behind the trench away from the bank, showed a fast response and a high water surface, indicating that water was also moving into the field as well as towards the bank. The fact that there was such a quick response between filling the trench and rise in the water surfaces of the deep wells indicates much of the water was moving quickly to the deep conductive layer. These deep wells indicate a hydraulic gradient of 0.3 m/m towards the streambank.

The water surface elevation of the 2 m wells indicated preferential flow in the vadose zone above the groundwater table (fig. 10). Well 9 was near the bank and the most eastward well. This well only varied by 0.10 m over the entire seepage experiment tests (3/14/2011 to 3/22/2011). On the other hand, well 7 (near the bank to the west) showed a strong response to the trench, varying by 0.64 m. Three tensiometers at 1.5 m lined the bank (BL150, BM150, and BR150). The westward tensiometer (BL150) had a greater response to the trench compared to the middle and right tensiometers (fig. 11). The hypothesized direction of primary flow is illustrated in figure 12 relative to the position of the tensiometers and observation wells.

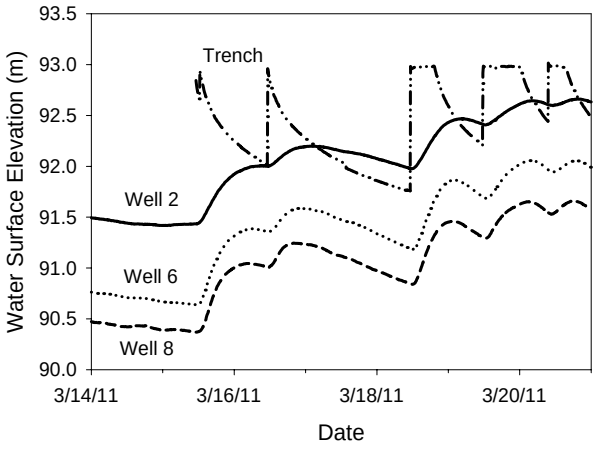

Figure 9. Water surface elevation of trench and 4.3 m wells.

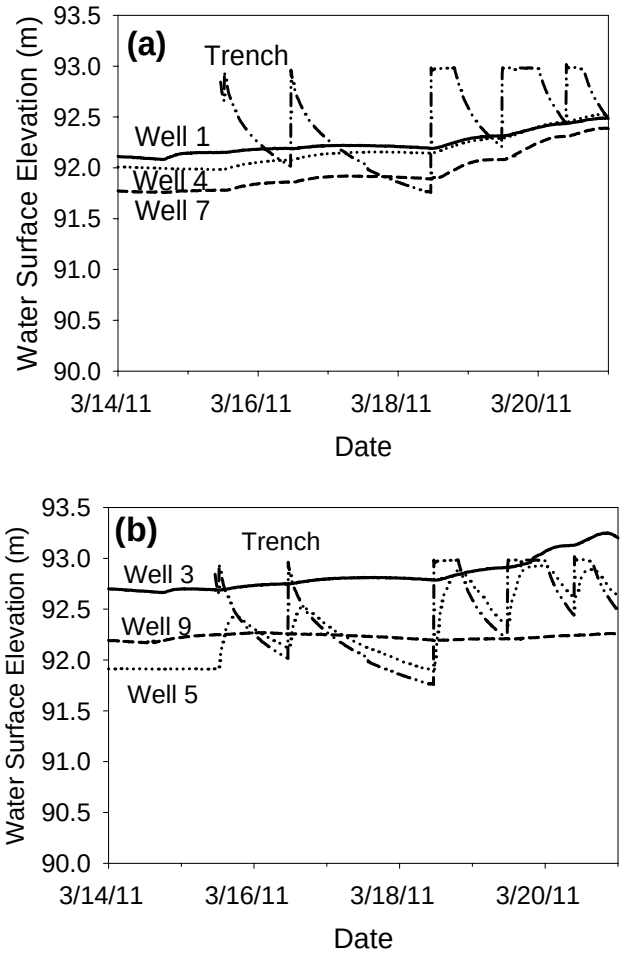

Figure 10. Water surface elevation of trench and 2 m wells on the (a) west column and (b) east column of the well field/tensiometer layout.

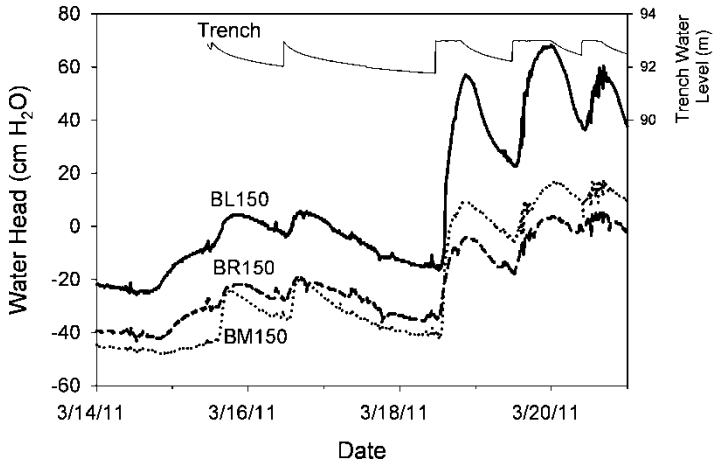

Figure 11. Soil-water pressures of three 150 cm tensiometers located nearest the bank. BL150 had the greatest response to the trench as shown by the three peaks after 3/18/2011.

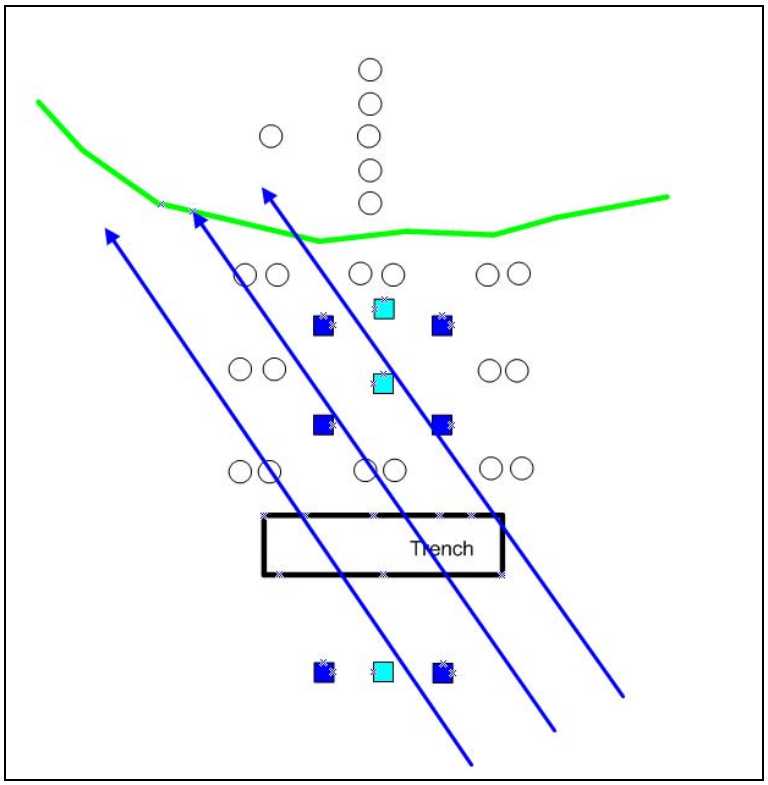

Figure 12. Site layout with blue arrows indicated predominate water flow direction.

Seepage Experiments

Table 3 provides an overview of the individual experiments and their maximum flow and erosion rates. The general method of failure was observed to be seepage of underlying non-cohesive sand followed by mass failure of upper cohesive soil. Seepage erosion and pop-out failures due to seepage gradient forces were both observed to be dominating forces of erosion in the sand layer. Generally the soil-water pressures of the upper cohesive material would also increase as indicated by tensiometers, thereby increasing the weight of the soil and eventually causing a mass failure event.

Each experiment described below would start with a clean vertical face (Table 3). As the sand seeped out and cohesive material collapsed, it would be more difficult for the seepage to pass through/around the cohesive blocks, thus creating a 'self-healing' process. Fox et al., 2006 reported that seepage erosion and fluvial erosion must be linked, or the accumulated sediment from seepage erosion and subsequent mass failure would both continue if fluvial erosion does not remove the failed material. Experiment two simulated this process of removal by fluvial erosion by manually removing all failed material. Such action greatly increased the erosion rate and growth in size of the undercut. This documents the importance of seepage erosion acting in concert with fluvial forces. The power of the self-healing process can be demonstrated in the undercut growth of the various seepage experiments. In the middle seep, undercut growth was 10 cm in depth over 8 hours. This is after the initial formation of a 30 cm deep undercut before sampling began. The WS1 experiment experienced much faster growth (38 cm in depth over 51 minutes). These experiments were characterized by rapid undercut growth initially then slowing

due to self-healing. The experiment for the west seep, in which failed material was removed, experienced 91 cm of growth in just 40 minutes.

Table 3. Overview of flow and erosion rates of each experiment.

Experiment Label	Description	Max Flowrate (L/min)	Avg. Flowrate (L/min)	Max Erosion Rate (g/min)	Avg. Erosion Rate (g/min)
MS (Middle Seep)	Seep was running, trench filled	0.43	0.29	7.85	1.78
ES (East Seep)	Trench filled and several hours later seep began	0.0059	0.005	0.134	0.055
WS1 (West Seep 1)	Trench not filled	0.40	0.24	864.58	194.01
WS2[a] (West Seep 2)	Trench not filled	2.16	1.38	6913.52	4214.41
LTE (Long Term Exp.)	Trench filled, observed for 2 days				

[a] WS2 is a special case experiment where failed material (either seeped or sapped) was removed immediately and counted towards the total erosion rates shown.

Middle Seep Experiment (MS)

The middle seep was observed to be flowing several days before the actual experiment due to a high water table caused by rain events combined with filling of the trench a few days previously. The trench was filled and samples started to be collected at 11:20 on the morning of 3/18/2011. The trench head was held constant at 1.4 m for eight hours once filled. Initially a vertical face was created at the seepage location. The flowrates started at 0.21 L/min and rose until a final flowrate of 0.42 L/min (fig. 13). Erosion rates also appeared to slightly increase with time. There were two observations (5.35 g/min and 7.85 g/min) which seemed to fall outside the general increasing trend between 0.81 g/min to 2.57 g/min, hypothesized to be due to small-scale failures of the overlying cohesive layers (fig. 13). Figure 14 shows the seep near the beginning and end of the experiment. After eight hours, the collection pan became overwhelmed with material blocking further particle mobilization.

East Seep Experiment (ES)

The east seepage location did not experience seepage until 5 hours into the experiment. This location was setup similar to middle seep with a vertical shear face and collection pan installed. Flowrates started at 0.004 L/min and slowly rose to a final flowrate of 0.006 L/min and erosion rates varied between 0.015 g/min to 0.134 g/min. This was a low flow seep location.

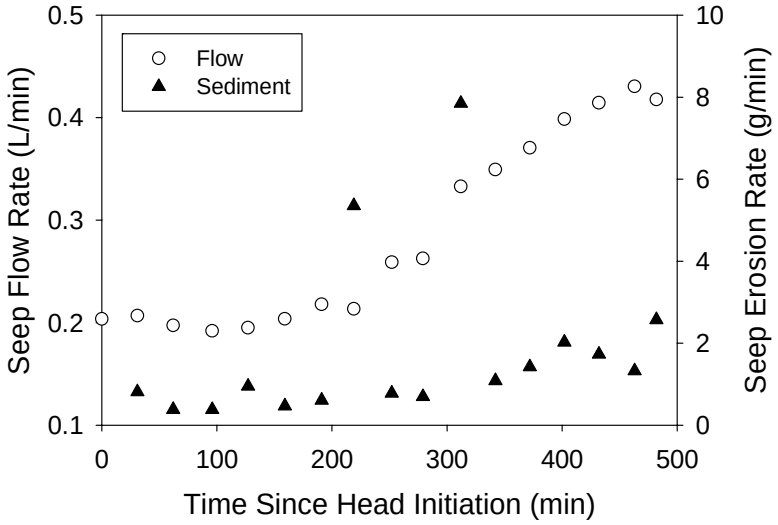

Figure 13. Seep flow and erosion rates versus time after initiation of a hydraulic head in the trench on the middle seep.

Figure 14. Middle seep near beginning of experiment (left) and near end of experiment (right).

West Seep Experiments

Once some toe material was removed and the pan installed, seepage began immediately in this location (fig. 15). Sampling of this seep occurred for 51 minutes when the collection pan became overwhelmed with cohesive material blocking continued particle mobilization (fig. 16). Flow rates were typically between 0.2 and 0.3 L/min with erosion rates peaking at one sampling time at greater than 800 g/min, again most likely due to a small-scale failure in the seepage undercut formation.

This second experiment on the west seepage location attempted to separate the seeped material from the mass failure material as fast as possible after failure, essentially removing the 'self-healing' aspect of the previous experiments. This resulted in high erosion rates creating a 3' deep cavity within 42 minutes. Seepage flow rates increased between 2.0 and 3.0 L/min due

to removal of the sediment from the undercut and erosion rates were orders of magnitude higher without the ‘self-healing’ process (fig. 17).

Figure 15. Picture of WS1 near beginning (left) and end (right) of experiment.

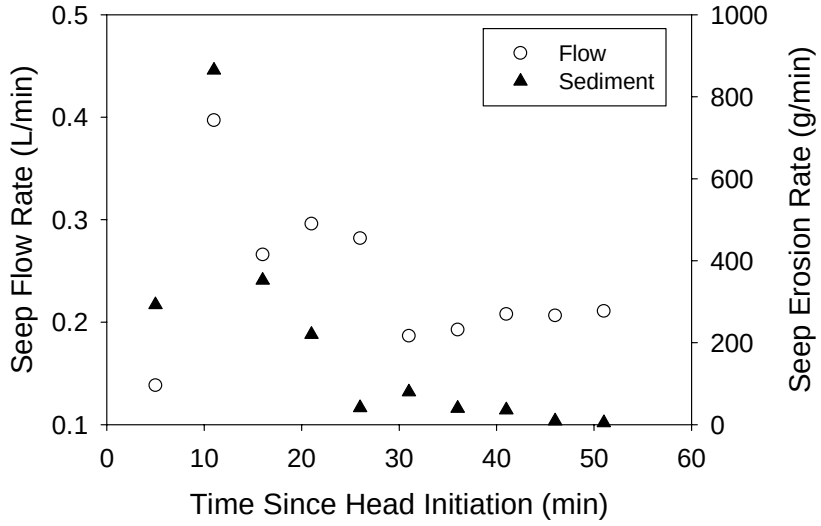

Figure 16. Flow and erosion rates versus time for WS1 (material allowed to remain in the collection flume) on the left streambank seep.

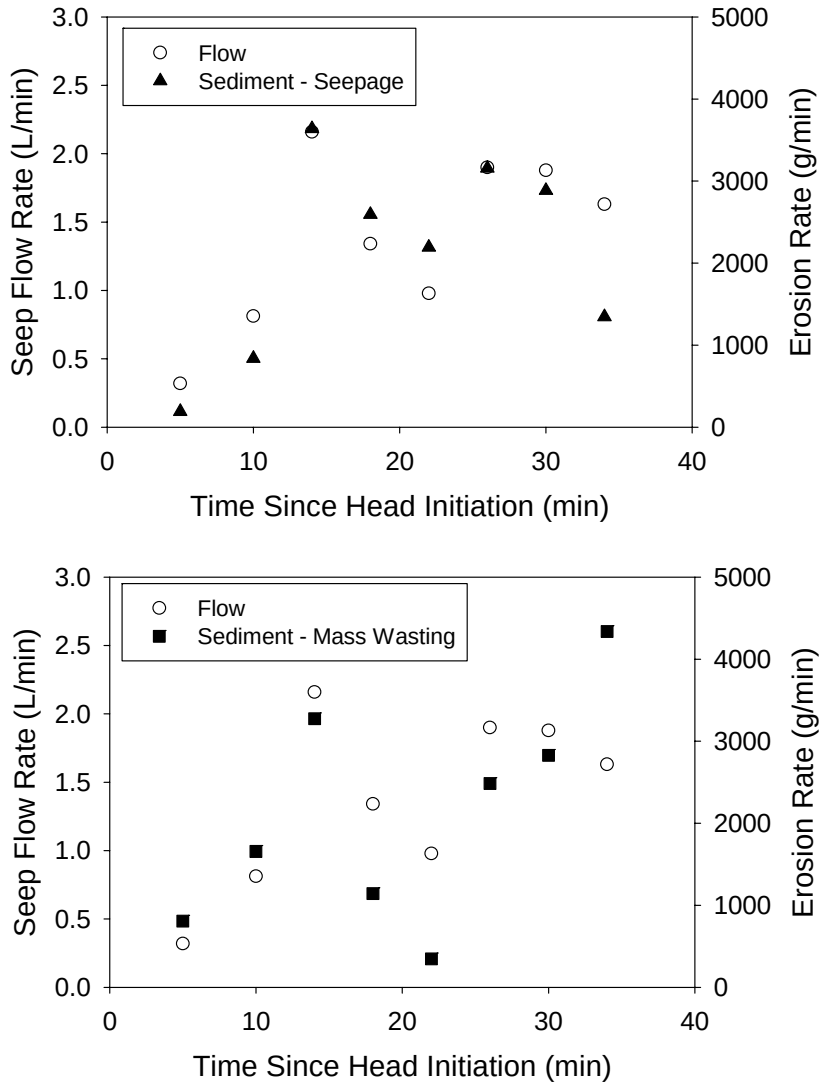

Figure 17. Seepage flow and erosion (seepage on top and mass wasting on bottom) rates over time for experiment two (sediment and mass wasting material removed from collection flume) on the right seep.

Long Term Experiment (LTE)

No samples were collected for this experiment, but the trench was filled and all three seepage locations were observed. A T5 tensiometer was moved to the cohesive material above the undercut created by the WS2 experiment (fig. 18). The tensiometer indicated saturation immediately and the soil-water pressure increased until a failure occurred between 12:50 pm and 12:52 pm (fig. 19).

Figure 18. Photos taken four minutes apart, before and after large failure of overhanging material over the west seep. The undercut was caused by WS2 experiment. Figure 19 shows the soil-water pressures of the failed material recorded by the T5 tensiometer visible in the pictures.

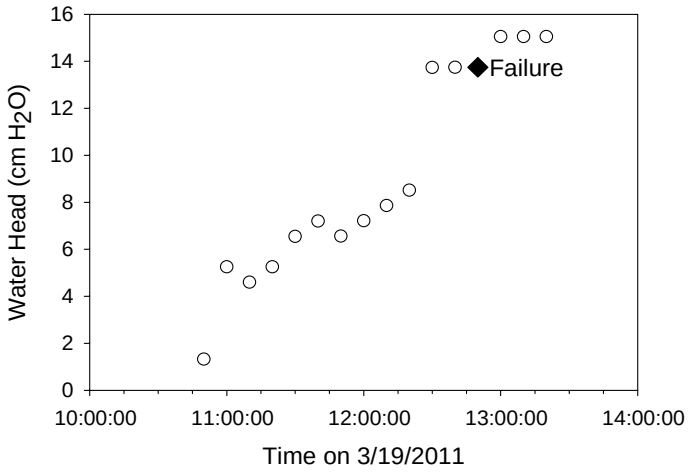

Figure 19. Soil-water pressure indicated by a T5 tensiometer inserted above undercut caused by previous experiment. Diamond indicates time of failure on 3/19/2011.

Conclusions

Seepage erosion mechanisms have been examined more extensively in the laboratory, but limited work has been conducted in the field to observe and quantify these mechanisms under controlled conditions. This research provided an innovative investigation into seepage flow and erosion measurements and mechanisms through the use of a trench injection system installed near a streambank face along Dry Creek in northern Mississippi. Seepage from the trench injections rapidly mobilized particles from the sand layer. Undercutting from the seepage erosion resulted in unstable upper cohesive banks. All three forms of erosion due to subsurface flow were observed. Seepage erosion of the sand was the dominate mechanism removing

sediment from the bank. Seepage gradient forces caused pop-out failures in the sand layer. The failed material would have to be mobilized by seepage flow to completely remove the sediment from the location or it blocks further mobilization. Increased soil-water pressures caused high soil weights in the cohesive layer above the sand layer. As seepage erosion undercutting progressed, blocks of cohesive soil would fail due to the increased weight and reduced support. These failures of cohesive soil acted as blockage to further seepage erosion and therefore healed the seeps. This is an example of seal-healing erosion. When these failures involved just the sand layer, seepage was able to entrain particles and self-healing did not prevent continued erosion. With this knowledge, it can be assumed that seepage erosion can be a dominate factor for streambank erosion when linked with fluvial erosion to remove the displaced sediment. For seepage erosion to continue apart from fluvial erosion. there must be enough force from the seepage flow to remove the cohesive 'capping' layer or occur where there is no upper layer cohesive material to 'block' the seeps. This work demonstrates the need for future work on fluvial erosion simultaneous with seepage erosion. Current research is underway investigating the effect of seepage gradients on the erodibility coefficient of soil, which could be a factor in many of these cases, and future work is planned to link fluvial and seepage erosion processes.

Acknowledgments

The authors wish to thank the technical support personnel at the National Sedimentation Laboratory in Oxford, MS for assistance with instrumentation and data collection for this project. This material is based upon work supported by the National Science Foundation under Grant No. 0943491. Any opinions, findings, and conclusions or recommendations expressed in this material are those of the authors and do not necessarily reflect the views of the National Science Foundation.

References

ASCE Task Committee on Hydraulics, Bank Mechanics, and Modeling of River Width Adjustment. 1998. River width adjustment. I: Processes and mechanisms. *J. Hydraul. Engr.-ASCE* 124(9):881-902.

Chu-Agor, M.L., G.A. Fox, R.M. Cancienne, and G.V. Wilson. 2008. Seepage caused tension failures and erosion undercutting of hillslopes. J. Hydrol. 359:247-259.

Fredlund, D.G., and H. Rahardjo. 1993. *Soil Mechanics for Unsaturated Soils*. John Wiley & Sons, New York.

Fox, G.A., G.V. Wilson, R.K. Periketi, and R.F. Cullum. 2006. Sediment Transport Model for Seepage Erosion of Streambank Sediment. *J. Hydrol. Engr.* 11(6):603-611.

Fox, G.A., G.V. Wilson, A Simon, E.J. Langendoen, O. Akay, and J.W. Fuchs. 2007. Measuring streambank erosion due to groundwater seepage: correlation to bank pore water pressure, precipitation and stream stage. *Earth Surface Processes and Landforms*. DOI:10.1002/esp.1490, 32:447-459.

Fox, G.A., and G.V. Wilson. 2010. The Role of Subsurface Flow in Hillslope and Stream Bank Erosion: A Review. *Soil Sci. Soc. Am. J.* 74:717-733.

Hagerty, D.J., M.F. Spoor, and C.R. Ullrich. 1981. Bank failure and erosion on the Ohio River. *Engr. Geol.* 17:141-158.

Hagerty, D.J. 1991. Piping/Sapping Erosion. I: Basic Considerations. J. Hydraul. Engr.-ASCE 117(8):991-1008.

Iverson, R.M., and J.J. Major. 1986. Groundwater Seepage Vectors and the Potential for Hillslope Failure and Debris Flow Mobilization. *Water Resour. Res.* 22(11):1543-1548.

Lawler, D.M., C.R. Thorne, and J.M. Hooke. 1997. Bank erosion and instability. In *Applied Fluvial Geomorphology for River Engineering and Management*, C.R. Thorne, R.D. Hey, and M.D. Newson (eds). John Wiley & Sons: New York, pp. 137-172.

Lobkovsky, A.E., B. Jensen, A. Kudrolli, and D.H. Rothman. 2004. Threshold phenomena in erosion driven by subsurface flow. *J. Geophysical Res.* 109:F04010, doi:10.1029/2004JF000172.

Richards, K.S., and K.R. Reddy. 2007. Critical appraisal of piping phenomena in earth dams. *Bull. Eng. Geol. Environ*. 66:381-402.

Rinaldi, M., N. Casagli, S. Dapporto, and A. Gargini. 2004. Monitoring and Modelling of Pore Water Pressure Changes and Riverbank Stability during Flow Events. *Earth Surf. Proc. Land.* 29:237-254.

Rulon, J.J., R. Rodway, and R.A. Freeze. 1985. The Development of Multiple Seepage Faces on Layered Slopes. *Water Resour. Res.* 21(11):1625-1636.

Wilson, G.V., R. Periketi, G.A. Fox, S. Dabney, D. Shields, and R.F. Cullum. 2007. Soil properties controlling seepage erosion contributions to streambank failure. *Earth Surf. Proc. Land.* 32(3):447-459.

Wilson, C.G., R.A. Kuhnle, D.D. Bosch, J.L. Steiner, P.J. Starks, M.D. Tomer, and G.V. Wilson. 2008. Quantifying relative contributions from sediment sources in Conservation Effects Assessment Project watersheds. *J. Soil Water Conserv.* 63(6):523-531.

Wilson, G.V., J. Nieber, and R.C. Sidle. 2011. Internal erosion during soil pipe flow: Role in gully erosion and hillslope instability. Proceedings: International Symposium on Erosion and Landscape Evolution, ASABE Specialty Conference, Anchorage, Alaska, Sept. 19-24, 2011.